JOURNAL OF GUIDANCE, CONTROL, AND DYNAMICS
Vol. 24, No. 2, March–April 2001

Optimal Bounded Low-Thrust Rendezvous with Fixed Terminal-Approach Direction

M. Guelman* and M. Aleshin†
Technion—Israel Institute of Technology, 32000 Haifa, Israel

The bounded, low-thrust, fixed-time, fuel-optimal constrained terminal approach direction rendezvous using the relative linearized equations of motion is investigated. A minimum fuel, two-stage solution is developed. In the first stage, optimal transfer from initial conditions to an intermediate point in the final line approach is implemented. In the second stage, an optimal thrust program guaranteeing directional approach is applied. Optimal rendezvous with fixed terminal approach is achieved by minimizing overall fuel consumption as a function of the intermediate point relative location and velocity in the final line approach. Solutions are generated and analyzed with final time as a parameter. Numerical results for a representative case are presented.

Introduction

THE potential of solar–electrical propulsion system for future space missions has been well recognized.[1] This propulsion system, which is characterized by variable exhaust velocity and limited power, produces low thrust with high specific impulse, greatly reducing the initial spacecraft mass. This mass reduction makes possible a new generation of small and sophisticated spacecraft for a variety of missions, from satellite station keeping to interplanetary missions, as well as maneuvers in the vicinity of space stations and even small comets or asteroids.

For efficiency, an optimal trajectory is desired. In most cases, the objective is to guide the spacecraft from an initial state to a final state (position and velocity), with minimum fuel expenditure. Optimal trajectory analyses of such systems were discussed in several comprehensive works, such as that by Marec.[2] Advanced analysis should consider practical issues, such as bounds on the thrust levels.

Optimum unbounded thrust rendezvous programs for power-limited propulsion systems were examined by Lembeck and Prussing[3] using equations linearized about a nominal circular orbit and by Carter[4] using equations linearized about general Keplerian orbits. Exact, analytical expressions were obtained for the required control accelerations. Pardis and Carter[5] and Kechichian[6] derived bounded, low-thrust rendezvous trajectories with power-limited propulsion systems. Carter and Pardis[7] extended the work for the case where the controller has both upper and lower bounds. To avoid saturation, they proposed the use of multiple engines, where each one has continuous thrust bounded by upper and lower limits.

In all of these works no constraints were imposed on the chaser's final approach to the target. However, the final approach of a real rendezvous is constrained. Proximity maneuvering is started at a certain distance from the target and is to be performed along the target-docking axis. Therefore, these path constraints at the final approach have to be taken into account to perform terminal approach along a prespecified inertial or target-relative direction.

In Ref. 8, a minimum fuel, two-stage solution was developed for the power-limited unbounded thrust rendezvous with a fixed final direction approach. In the first stage, optimal transfer from initial conditions to an intermediate point in the final line approach was implemented. In the second stage, an optimal thrust program guaranteeing directional approach was applied. Optimal rendezvous with fixed terminal approach was achieved by minimizing overall fuel consumption as a function of the intermediate point relative location and velocity in the final line approach. This two-stage solution will be now extended for the case of a power-limited bounded thrust rendezvous with fixed final approach direction.

Received 11 March 1999; revision received 24 July 2000; accepted for publication 2 August 2000.

*Professor, Faculty of Aerospace Engineering, Technion City. Member AIAA.
†Graduate Student, Faculty of Aerospace Engineering.

Problem Statement

A maneuvering chase vehicle is initially located at a small relative distance (compared to the orbital radius) from a passive target. The target vehicle is in circular orbit about a planet. A low-thrust, power-limited system is to be used by the chaser to execute efficiently a terminal rendezvous maneuver. To study this problem, the linearized equations about a nominal orbit will be employed. These equations are commonly referred to as the Clohessy–Wiltshire (CW) equations.

The CW rotating coordinate frame is fixed in the target spacecraft with the origin moving at a constant angular velocity given by the mean motion n. This rotating coordinate system is shown in Fig. 1 with y in the direction of the radius vector, x in the negative velocity vector direction, and z is the out-of-plane displacement in the direction of the frame rotation vector.

The CW equations are[9]

$$\ddot{x}(t) = 2n\dot{y}(t) + \Gamma_x \tag{1}$$

$$\ddot{y}(t) = -2n\dot{x}(t) + 3n^2 y(t) + \Gamma_y \tag{2}$$

$$\ddot{z}(t) = -n^2 z(t) + \Gamma_z \tag{3}$$

where Γ_x, Γ_y, and Γ_z are the thrust acceleration components.

When normalized, canonical units are employed, the spacecraft equations of motion can be written compactly in terms of relative position and velocity vectors $\boldsymbol{r}^T = [x \;\; y \;\; z]$ and $\boldsymbol{v}^T = [\dot{x} \;\; \dot{y} \;\; \dot{z}]$ as

$$\begin{pmatrix} \dot{\boldsymbol{r}} \\ \dot{\boldsymbol{v}} \end{pmatrix} = \begin{pmatrix} 0 & I \\ A_1 & A_2 \end{pmatrix} \begin{pmatrix} \boldsymbol{r} \\ \boldsymbol{v} \end{pmatrix} + \begin{pmatrix} 0 \\ \boldsymbol{\Gamma} \end{pmatrix} \tag{4}$$

where 0 and I are 3×3 zero and identity matrices, respectively, and the matrices A_1 and A_2 are defined by

$$A_1 = \begin{pmatrix} 0 & 0 & 0 \\ 0 & 3 & 0 \\ 0 & 0 & -1 \end{pmatrix}, \qquad A_2 = \begin{pmatrix} 0 & 2 & 0 \\ -2 & 0 & 0 \\ 0 & 0 & 0 \end{pmatrix} \tag{5}$$

For minimum fuel in a power-limited system, it is required to minimize the performance index[2]

$$J = \frac{1}{2} \int_{t_0}^{t_f} \boldsymbol{\Gamma}^T \boldsymbol{\Gamma} \, \mathrm{d}t \tag{6}$$

where t_0 and t_f are fixed initial and final times and $\boldsymbol{\Gamma}$ is the thrust-acceleration vector with

$$|\Gamma(t)| \leq \Gamma_{\max} \tag{7}$$

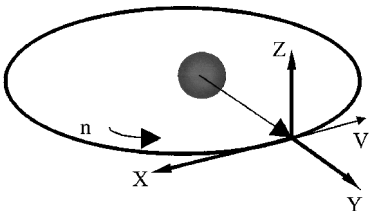

Fig. 1 CW coordinate frame.

with $\Gamma_{\max}$ a positive real number expressing the upper bound on the thrust-acceleration magnitude. The mass change due to fuel consumption over the flight interval is assumed to be insignificant and, therefore, constrained maximum thrust-acceleration is used instead of a constrained maximum thrust level.

Optimal solutions for power-limited systems with upper bound[5,6] and both upper and lower bounds on thrust magnitude[7] were investigated. Multiple thrusters and discrete thrust level[10] solutions were also considered. In the present paper, we restrict ourselves to the case of an upper bound on the thrust magnitude and its effects on rendezvous with fixed terminal approach direction.

Let the final approach direction be defined by unit vector $\boldsymbol{u} = [u_x \;\; u_y \;\; u_z]^T$. Given a final direction approach unit vector $\boldsymbol{u}$ expressed in the rotating CW frame, the constrained final direction minimum fuel can be defined as follows: Given initial conditions $\boldsymbol{r}(t_0)$ and $\boldsymbol{v}(t_0)$ find the thrust control acceleration vector $\boldsymbol{\Gamma}$ to achieve final conditions $\boldsymbol{r}(t_f) = \boldsymbol{0}$ and $\boldsymbol{v}(t_f) = \boldsymbol{0}$ at given final time t_f such that for $t \to t_f$, $\boldsymbol{r}(t) \times \boldsymbol{u} \to 0^+$ and $\boldsymbol{v}(t) \times \boldsymbol{u} \to 0^+$, while the performance index J is minimized.

Note that the vector cross-product requirements on both the relative position and velocity vectors represent in qualitative terms the terminal approach constraint conditions. The actual conditions imposed to achieve the final approach constraint are defined later in the paper.

Optimal Control

Given equations of motion (4) and the performance index (6), the Hamiltonian function is

$$H = \tfrac{1}{2}\Gamma^2 + \boldsymbol{\lambda}_r^T \boldsymbol{v} + \boldsymbol{\lambda}_v^T (A_1 \boldsymbol{r} + A_2 \boldsymbol{v} + \boldsymbol{\Gamma}) \tag{8}$$

The adjoint equations are

$$\dot{\boldsymbol{\lambda}}_r = -A_1^T \lambda_v \tag{9}$$

$$\dot{\boldsymbol{\lambda}}_v = -A_2^T \boldsymbol{\lambda}_v - \boldsymbol{\lambda}_r \tag{10}$$

When the minimum principle is applied, the Hamiltonian is minimized by

$$\boldsymbol{\Gamma}^*(t) = \begin{cases} -\boldsymbol{\lambda}_v(t) & |\boldsymbol{\lambda}_v(t)| \le \Gamma_{\max} \\ [-\Gamma_{\max}/|\boldsymbol{\lambda}_v(t)|]\boldsymbol{\lambda}_v(t) & |\boldsymbol{\lambda}_v(t)| \ge \Gamma_{\max} \end{cases} \tag{11}$$

State and adjoint equations can be written compactly as

$$\begin{pmatrix} \dot{\boldsymbol{r}} \\ \dot{\boldsymbol{v}} \\ \dot{\boldsymbol{\lambda}}_r \\ \dot{\boldsymbol{\lambda}}_v \end{pmatrix} = \begin{pmatrix} 0 & I & 0 & 0 \\ A_1 & A_2 & 0 & -h(t) \\ 0 & 0 & 0 & -A_1^T \\ 0 & 0 & -I & -A_2^T \end{pmatrix} \begin{pmatrix} \boldsymbol{r} \\ \boldsymbol{v} \\ \boldsymbol{\lambda}_r \\ \boldsymbol{\lambda}_v \end{pmatrix} \tag{12}$$

where

$$h(t) = \begin{cases} 1 & |\boldsymbol{\lambda}_v(t)| \le \Gamma_{\max} \\ [\Gamma_{\max}/|\boldsymbol{\lambda}_v(t)|] & |\boldsymbol{\lambda}_v(t)| \ge \Gamma_{\max} \end{cases} \tag{13}$$

Equation (12) represents a set of nonlinear differential equations.

Unbounded-Control Synthesis

For the case of unbounded thrust acceleration, state and adjoint equations can be written as

$$\begin{pmatrix} \dot{\boldsymbol{r}} \\ \dot{\boldsymbol{v}} \\ \dot{\boldsymbol{\lambda}}_r \\ \dot{\boldsymbol{\lambda}}_v \end{pmatrix} = \begin{pmatrix} 0 & I & 0 & 0 \\ A_1 & A_2 & 0 & -I \\ 0 & 0 & 0 & -A_1^T \\ 0 & 0 & -I & -A_2^T \end{pmatrix} \begin{pmatrix} \boldsymbol{r} \\ \boldsymbol{v} \\ \boldsymbol{\lambda}_r \\ \boldsymbol{\lambda}_v \end{pmatrix} \tag{14}$$

As can be seen from Eq. (14), the system is linear, the adjoint equations can be solved separately from the state equations, and furthermore the transition matrix for the adjoint vector is the same as for the unthrusted state equations.[3]

Solution of the adjoint equations is given by the adjoint transition matrix Φ_λ as

$$\begin{bmatrix} \boldsymbol{\lambda}_r(t) \\ \boldsymbol{\lambda}_v(t) \end{bmatrix} = \Phi_\lambda(t - t_0)\boldsymbol{\lambda}_0 \tag{15}$$

where $\boldsymbol{\lambda}_0 = [\boldsymbol{\lambda}_r^T, \boldsymbol{\lambda}_v^T]^T$ is the adjoint initial condition vector. When the matrix Φ_λ is partitioned into two submatrices as

$$\Phi_\lambda(t - t_0) \triangleq \begin{bmatrix} \Phi_{\lambda r}(t - t_0) \\ \hline \Phi_{\lambda v}(t - t_0) \end{bmatrix} \tag{16}$$

and Eq. (11) is utilized, the optimal thrust-acceleration vector is given by

$$\boldsymbol{\Gamma}^*(t) = -\Phi_{\lambda v}\boldsymbol{\lambda}_0 \tag{17}$$

The solution for the position-velocity state vector due to the optimal thrust acceleration is

$$\boldsymbol{x}(t) = \Phi(t - t_0)\boldsymbol{x}(t_0) + \Psi(t - t_0)\boldsymbol{\lambda}_0 \tag{18}$$

where Ψ is the convolution integral for the position-velocity state vector due to the optimal thrust acceleration $\Gamma^*(t)$. Vector $\boldsymbol{\lambda}_0$ is defined such that the boundary conditions are fulfilled.

For the free approach-direction rendezvous, $\boldsymbol{\lambda}_0$ is defined by[3]

$$\boldsymbol{\lambda}_0 = -\Psi^{-1}(t_f - t_0)\Phi(t_f - t_0)\boldsymbol{x}(t_0) \tag{19}$$

To solve the problem of rendezvous with a final approach direction, it would appear that the simplest solution is to determine terminal boundary conditions by

$$\boldsymbol{r}(t_f) = -\varepsilon \begin{pmatrix} u_x \\ u_y \\ u_z \end{pmatrix}, \qquad \boldsymbol{v}(t_f) = \delta \begin{pmatrix} u_x \\ u_y \\ u_z \end{pmatrix} \tag{20}$$

instead of $\boldsymbol{r}(t_f) = \boldsymbol{0}$ and $\boldsymbol{v}(t_f) = \boldsymbol{0}$, where ε and δ are small values defining the final relative position and velocity, respectively. Vector $\boldsymbol{\lambda}_0$ satisfying the boundary conditions is defined by

$$\boldsymbol{\lambda}_0 = -\Psi^{-1}(t_f - t_0)[\Phi(t_f - t_0)\boldsymbol{x}(t_0) - \boldsymbol{x}(t_f)] \tag{21}$$

This solution was implemented in Ref. 8. The chaser spacecraft effectively reaches the target spacecraft along the required final approach direction; however, it is only near the final point that the required terminal boundary conditions are satisfied. This follows because when the required turning rates are implemented to modify both the velocity and flight directions, the optimal policy is to wait until the velocity magnitude approaches zero, requiring then only a negligible acceleration with a minimum cost.

To achieve the desired final approach direction from a sufficiently great range, a possible approach is to modify the performance index. To remain within the standard linear quadratic problem, the performance index is modified to include the squared distance from the chaser position to the desirable line, that is,

$$J_1 = \frac{1}{2}\int_{t_1}^{t_f} (\boldsymbol{\Gamma}^T \boldsymbol{\Gamma} + \alpha \boldsymbol{r}^T D \boldsymbol{r})\, \mathrm{d}t \tag{22}$$

where the matrix D is

$$D = \begin{pmatrix} u_y^2 + u_z^2 & -u_x u_y & -u_x u_z \\ -u_x u_y & u_x^2 + u_z^2 & -u_y u_z \\ -u_x u_z & -u_y u_z & u_x^2 + u_y^2 \end{pmatrix} \tag{23}$$

and α is a weighting coefficient. The matrix D is constant for the case of a fixed target-relative approach direction and is time varying for the case of a fixed inertial approach direction.

State and adjoint equations are now given by

$$\begin{pmatrix} \dot{\boldsymbol{r}} \\ \dot{\boldsymbol{v}} \\ \dot{\boldsymbol{\lambda}}_r \\ \dot{\boldsymbol{\lambda}}_v \end{pmatrix} = \begin{pmatrix} 0 & I & 0 & 0 \\ A_1 & A_2 & 0 & -I \\ -\alpha D & 0 & 0 & -A_1^T \\ 0 & 0 & -I & -A_2^T \end{pmatrix} \begin{pmatrix} \boldsymbol{r} \\ \boldsymbol{v} \\ \boldsymbol{\lambda}_r \\ \boldsymbol{\lambda}_v \end{pmatrix} \tag{24}$$

The adjoint equations can not be solved separately in this case. The thrust-acceleration vector $\boldsymbol{\Gamma}(t)$ that satisfies the minimum principle now depends on the relative position $\boldsymbol{r}(t)$ of the chaser. Numerical solutions were obtained,[8] and the result was that indeed the required direction is achieved. However, the quadratic cost function component, or any other quadratic form, has a major limitation: It leads to a nonsensitive sign solution. Only the terminal approach direction can be guaranteed, but not the desirable side. The spacecraft's final approach direction will depend on the initial boundary conditions and time interval. Both the side and direction can be achieved depending on the initial boundary conditions.

The approach taken to ensure the required final approach direction from a sufficiently great range is to employ a two-stage solution. The problem is solved by employing first an optimal transfer with performance index J, from the initial boundary conditions $\boldsymbol{x}(t_0) = [\boldsymbol{r}(t_0)^T, \boldsymbol{v}(t_0)^T]^T$ to an intermediate state-space point $\boldsymbol{x}(t_1)$, followed by a constrained directional approach that employs the performance index J_1.

The cost of the two-stage constrained rendezvous is the sum of the propellant costs for the transfer and proximity stages. Total fuel cost for a fixed final time is minimized by an adequate choice of the intermediate point $\boldsymbol{x}(t_1)$. Parameters defining the intermediate state-space point, as well as the stage braking time t_1, have to be obtained to minimize total fuel consumption for fixed mission time t_f.

The adopted solution defines first-stage final conditions such that the chaser will be on the final approach line at distance R with relative velocity amplitude V along the same line, that is,

$$\boldsymbol{x}(t_1) = [-R\boldsymbol{u}^T, V\boldsymbol{u}^T]^T \tag{25}$$

These are in turn the second-stage initial conditions.

Bounded-Thrust Rendezvous

The two-stage, low-thrust solution is applied now for the bounded thrust. Given equations of motion (4) and the performance indexes (6) and (22) for the first and second stages, respectively, the Hamiltonian function is minimized for both stages applying the same thrust acceleration as defined by Eq. (13). The state and adjoint equations for each stage can be written compactly as

$$\begin{pmatrix} \dot{\boldsymbol{r}} \\ \dot{\boldsymbol{v}} \\ \dot{\boldsymbol{\lambda}}_r \\ \dot{\boldsymbol{\lambda}}_v \end{pmatrix} = \begin{pmatrix} 0 & I & 0 & 0 \\ A_1 & A_2 & 0 & -h(t) \\ -\alpha(D) & 0 & 0 & -A_1^T \\ 0 & 0 & -I & -A_2^T \end{pmatrix} \begin{pmatrix} \boldsymbol{r} \\ \boldsymbol{v} \\ \boldsymbol{\lambda}_r \\ \boldsymbol{\lambda}_v \end{pmatrix} \tag{26}$$

where the weighting coefficient α multiplying the matrix D is zero for the first stage. Equation (26) represents a set of nonlinear differential equations. Because of the nonlinear form of the optimal thrust acceleration, the two-point boundary value problem is now solved for each stage numerically. The adjoint initial conditions for each stage, $\boldsymbol{\lambda}_0 = (\boldsymbol{\lambda}_{r0}^T, \boldsymbol{\lambda}_{v0}^T)^T$, satisfying the nonlinear Eq. (26), are found numerically in an iterative manner by a gradient method (the MATLAB® fsolve routine was implemented for the numerical solution).

The analytical solution for unsaturated thrust is taken as the initial guess for the adjoint initial conditions. The adjoint equations are unstable for forward integration and, therefore, divergence is expected during numerical integration of Eqs. (26) for the first stage, where the flight interval is sufficiently great. Analytical expressions obtained for the adjoint equations given in the Appendix and depending only on $\boldsymbol{\lambda}_0$ are used for the first-stage solution eliminating the adjoint equation's numerical integration.

As a representative example of a two-dimensional rendezvous, the case of a target spacecraft in a circular low Earth orbit at an altitude of 480 km is considered. The chaser spacecraft's initial position is 15 km behind the target with an initial relative velocity of 10 m/s in the negative X direction. The required terminal approach direction is the $+V$ bar or approach along the negative target velocity direction. Maximum thrust-acceleration magnitude taken for this numerical example is $\Gamma_{\max} = 5 \times 10^{-4}$ m/s^2. Such thrust-acceleration levels are currently available in electric propulsion systems. To achieve a solution for given maximum thrust-acceleration magnitude, the flight interval was taken to be 11 orbital periods. The weighting coefficient α for the second stage is in normalized units equal to 5×10^3. The intermediate point parameters are $R = 300$ m and $V = 0.2$ m/s for unsaturated second-stage flight. Figure 2 shows the relative optimal trajectory in the x–y plane. Figure 3 shows a close up of the final approach. As can be clearly seen, rendezvous is achieved along the required final approach direction. The required thrust acceleration for the first and second stages is shown in Figs. 4 and 5, respectively. As can be seen, the required thrust is almost fully saturated. The first- and second-stage fuel costs are $J_1 = 5.1342 \times 10^{-3}$ and $J_2 = 1.538 \times 10^{-4}$, respectively, for a total

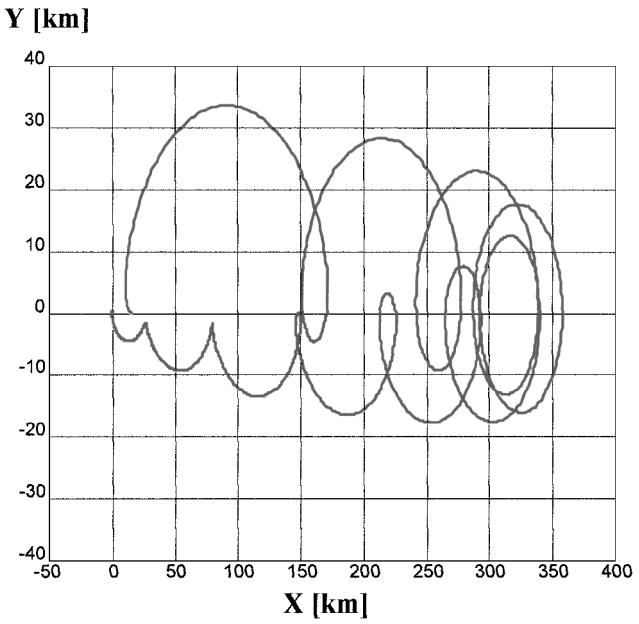

Fig. 2 Bounded thrust optimal trajectory.

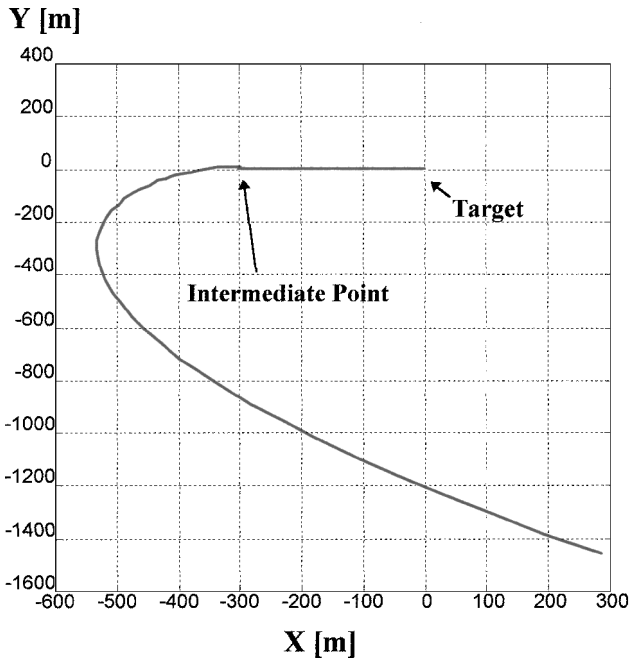

Fig. 3 Final approach relative trajectory.

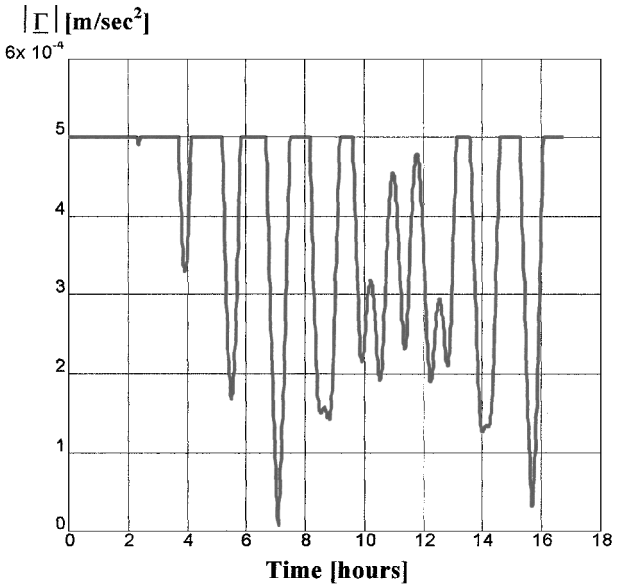

Fig. 4 First-stage optimal thrust acceleration.

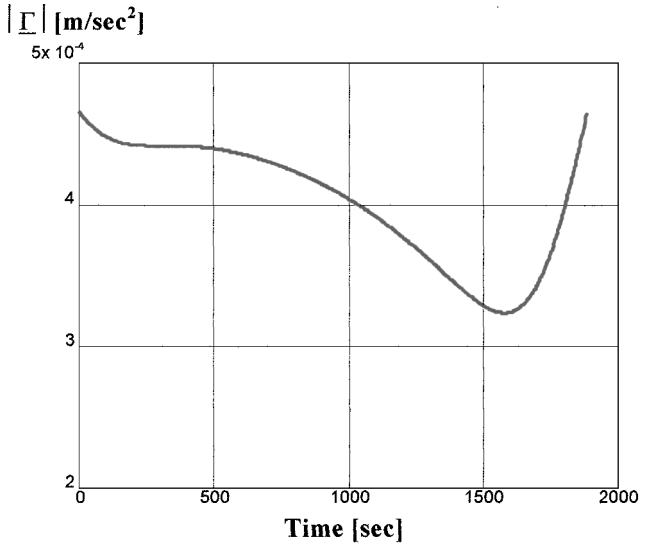

Fig. 5 Second-stage optimal thrust acceleration.

fuel cost of $J = 5.288 \times 10^{-3}$. For comparison purposes, the corresponding fully unsaturated first-stage cost is $J = 4.56 \times 10^{-3}$. The second-stage flight interval is 1885 s.

As a representative example of three-dimensional rendezvous, the same case of a target spacecraft in a circular low Earth orbit at an altitude of 480 km is considered. Now, the chaser spacecraft's initial conditions $\boldsymbol{r}_0 = [15, 0, 2]^T$ km and $\boldsymbol{v}_0 = [-10, 0, -2]^T$ m/s, are chosen outside the trajectory plane. The required terminal approach direction is again the $+V$ bar or approach along the negative target velocity direction. The flight interval is taken to be two orbital periods, and the weighting coefficient α for the second stage is equal to 5×10^3 in normalized units. The intermediate point parameters are $R = 300$ m and $V = 0.35$ m/s. Figure 6 shows the relative optimal trajectory and Fig. 7 shows a close up of the final approach. As can be clearly seen, the chaser successfully reaches the trajectory plane at the intermediate point. Rendezvous along the required final approach direction is achieved at the second stage. The required thrust accelerations for the first and second stages are shown in Figs. 8 and 9, respectively. Total fuel cost is $J = 2.995 \times 10^{-2}$. For comparison, the corresponding unconstrained terminal approach rendezvous cost is $J = 2.90 \times 10^{-2}$.

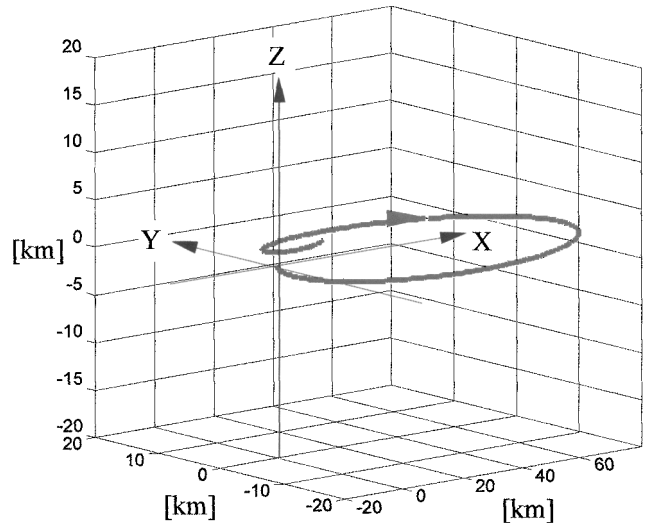

Fig. 6 Unbounded thrust three-dimensional optimal trajectory.

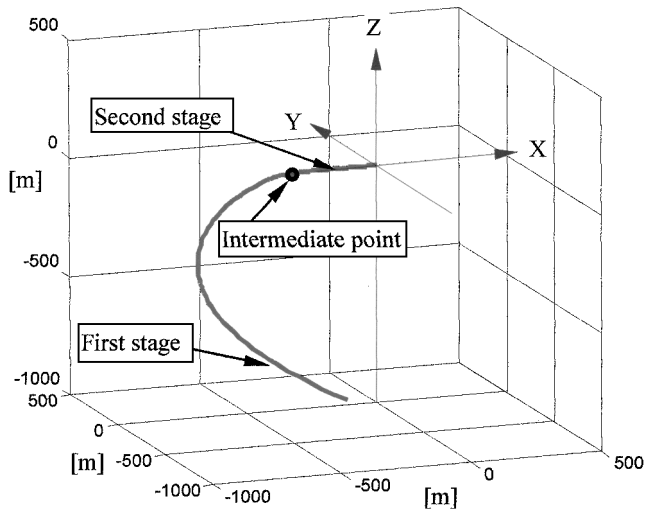

Fig. 7 Three-dimensional final approach relative trajectory.

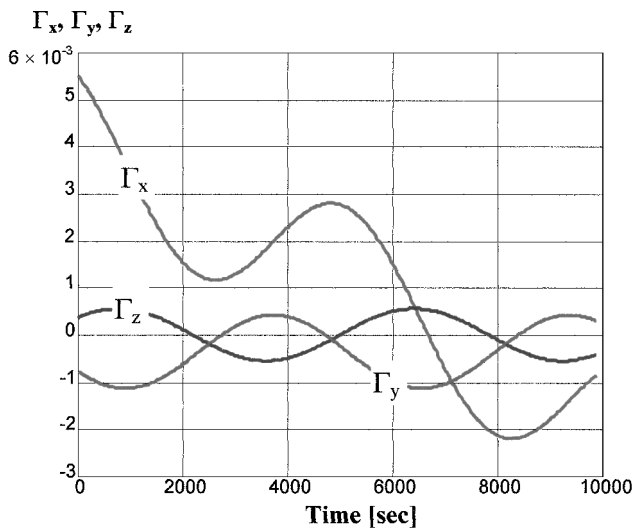

Fig. 8 Three-dimensional first-stage optimal thrust acceleration.

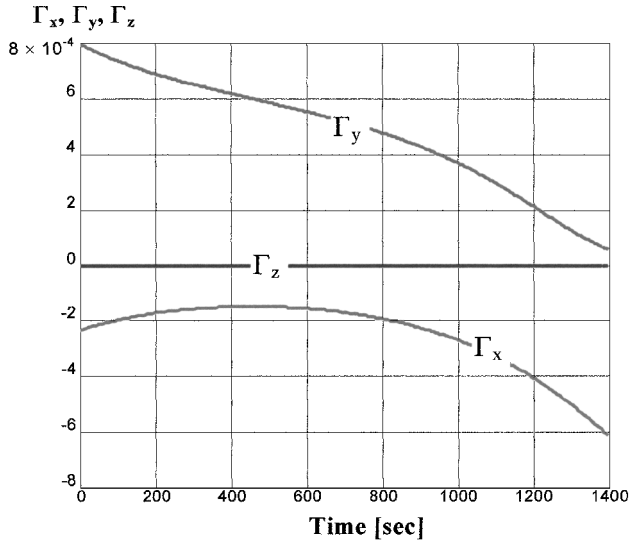

Fig. 9 Three-dimensional second-stage optimal thrust acceleration.

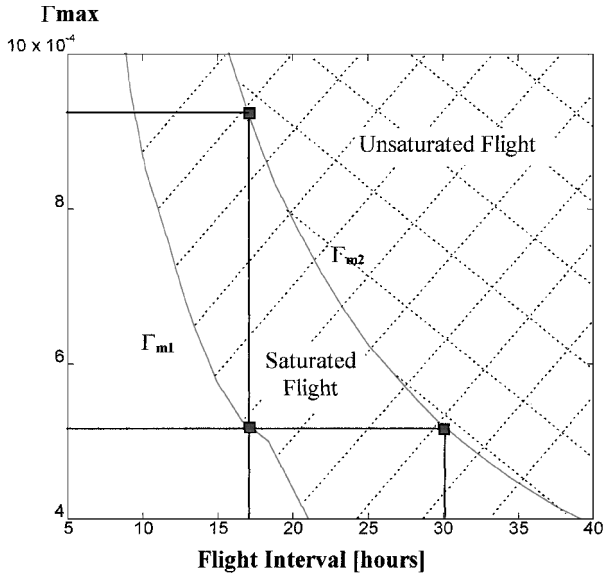

Fig. 10 First-stage maximum thrust for saturated and unsaturated flight.

Maximum Thrust and Cost Dependence on Flight Interval

In Ref. 5, the existence of a solution to the power-limited rendezvous with thrust saturation and the fuel consumed in an optimal solution as a function of the thrust magnitude was studied. A necessary condition for a solution to exist and a necessary and sufficient condition for an optimal solution to be fuel efficient, both in terms of the bound on thrust and the boundary conditions, were derived. A similar analysis will now be performed for the two-stage rendezvous with a fixed final approach direction. This analysis will be performed for the two stages separately because different requirements apply.

First Stage

For given boundary conditions for the first stage, the bound on the thrust for the existence of a solution is now determined as a function of the flight interval.

The set of bounded thrust admissible controls is a subset of the unbounded thrust admissible controls. It follows then that[5]

$$J_{\text{unsat}}(\Delta t) \le J_{\text{sat}}(\Delta t) \le J_{\text{tot}}(\Delta t) \tag{27}$$

where $\Delta t = (t_f - t_0)$ is the flight interval, J_{unsat} the cost of unsaturated flight, J_{sat} the cost of the flight with regions of saturation, and J_{tot} the cost of the totally saturated flight given by

$$J_{\text{tot}} = \tfrac{1}{2}\Gamma_{\max}^2 \Delta t \tag{28}$$

The expression for unsaturated flight cost function now will be derived. When the expression for optimal thrust acceleration given by Eq. (17) is utilized, the unsaturated flight cost as defined in Eq. (6) can be written as a quadratic form of the adjoint initial conditions as

$$J_{\text{unsat}} = \tfrac{1}{2}\boldsymbol{\lambda}_0^T \Omega(\Delta t)\boldsymbol{\lambda}_0 \tag{29}$$

where

$$\Omega(\Delta t) = \int_{t_0}^{t_f} \Phi_{\lambda v}^T \Phi_{\lambda v}\, \mathrm{d}t \tag{30}$$

and the adjoint initial conditions $\boldsymbol{\lambda}_0$ are given by Eq. (19). Now when Eqs. (28) and (29) are substituted into inequality (27), it follows that

$$\tfrac{1}{2}\boldsymbol{\lambda}_0^T \Omega(\Delta t)\boldsymbol{\lambda}_0 \le J(t) \le \tfrac{1}{2}\Gamma_{\max}^2 \Delta t \tag{31}$$

The necessary condition for the bounded thrust solution to exist is

$$\Gamma_{\max} \ge \Gamma_{m1} = \left(\frac{\boldsymbol{\lambda}_0^T \Omega(\Delta t)\boldsymbol{\lambda}_0}{\Delta t}\right)^{\frac{1}{2}} \tag{32}$$

where Γ_{m1} is a function of flight interval and is shown in Fig. 10.

Saturation is avoided during the flight if the maximum value of the optimal thrust-acceleration magnitude over the entire flight interval is smaller than the available maximum thrust-acceleration magnitude:

$$\max_{t_0 \le t \le t_f} |\boldsymbol{\Gamma}^*(t)| \le \Gamma_{\max} \tag{33}$$

Because the optimal thrust acceleration is given by $\boldsymbol{\Gamma}^*(t) = -\Phi_{\lambda v}(t)\boldsymbol{\lambda}_0$, the necessary and sufficient condition for the bounded thrust solution to be unsaturated is defined as

$$\max_{t_0 \le t \le t_f} \boldsymbol{\lambda}_0^T \left[\Phi_{\lambda v}^T(t)\Phi_{\lambda v}(t)\right]\boldsymbol{\lambda}_0 \le \Gamma_{\max}^2 \tag{34}$$

Typically, the global maximum occurs for $t = 0$, and a simple expression is obtained because the transition matrix becomes the identity matrix:

$$\boldsymbol{\lambda}_{v0}^T \boldsymbol{\lambda}_{v0} \le \Gamma_{\max}^2 \tag{35}$$

Because for each flight interval the adjoint initial conditions $\boldsymbol{\lambda}_0 = (\boldsymbol{\lambda}_{r0}^T, \boldsymbol{\lambda}_{v0}^T)^T$ are required to satisfy boundary conditions (25) along with nonlinear equations (26), $\Gamma_{m2} = \sqrt{(\boldsymbol{\lambda}_{v0}^T \boldsymbol{\lambda}_{v0})}$ is also a function of the flight interval. Γ_{m2} is shown in Fig. 10.

Given $\Gamma_{\max}$ and the boundary conditions, the minimal flight time interval $\Delta t_{\min}$ guaranteeing unsaturated flight can be derived numerically from Eq. (35). When the boundary conditions of the first stage of the particular numerical example where $\Gamma_{\max} = 5 \times 10^{-4}$ m/s^2 are substituted, the minimum flight time interval for unsaturated flight is obtained as $\Delta t_{\min} = 31$ h or about 21 orbital periods.

Fuel consumption is a function of flight interval. For the same case already considered, the total flight interval is varied from unsaturated flight region to totally saturated flight, and the resulting cost function as a function of flight interval is presented in Fig. 11.

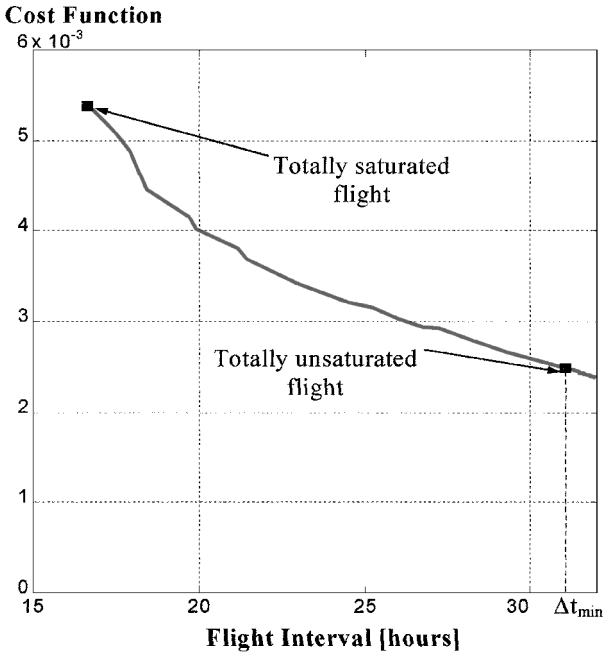

Fig. 11 First-stage cost function vs flight interval.

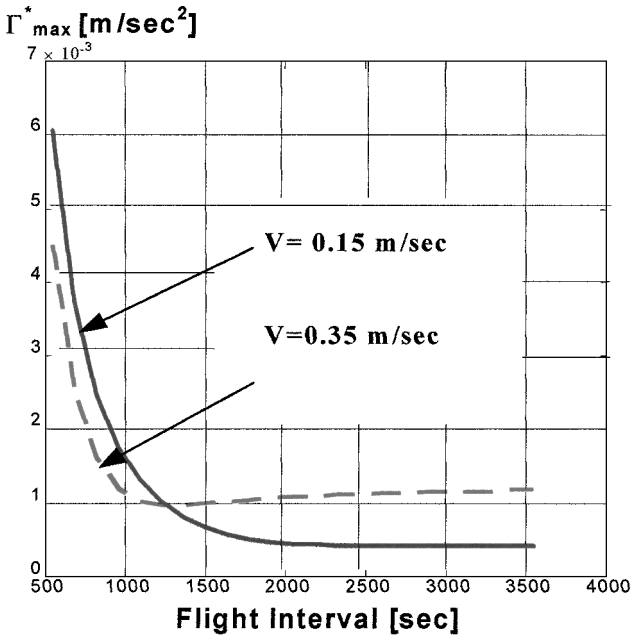

Fig. 12 Second-stage maximum thrust acceleration as a function of second-stage flight interval.

As can be seen in Figure 11, the first-stage cost for totally saturated flight is about twice that corresponding to unsaturated flight with the minimum possible flight interval. Note that with saturated flight, mission time can be decreased approximately to half, as can be seen from the Fig. 11. Thus, flight interval could be lengthened until the unsaturated flight region for better fuel economy is achieved, or alternatively, the same rendezvous mission could be performed in a shorter time at the expense of larger fuel consumption.

Second Stage

The second stage assures the constrained terminal approach. Because additional thrust acceleration is required for constrained terminal approach, the shorter the range at which the second stage is initialized the smaller is the cost. The actual value of second-stage initial range R, thus, can be defined only from safety requirements.

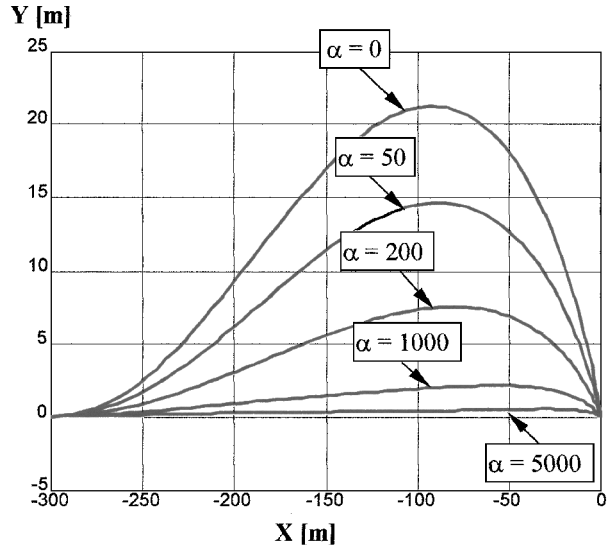

Fig. 13 Optimal second-stage rendezvous trajectories as function of α.

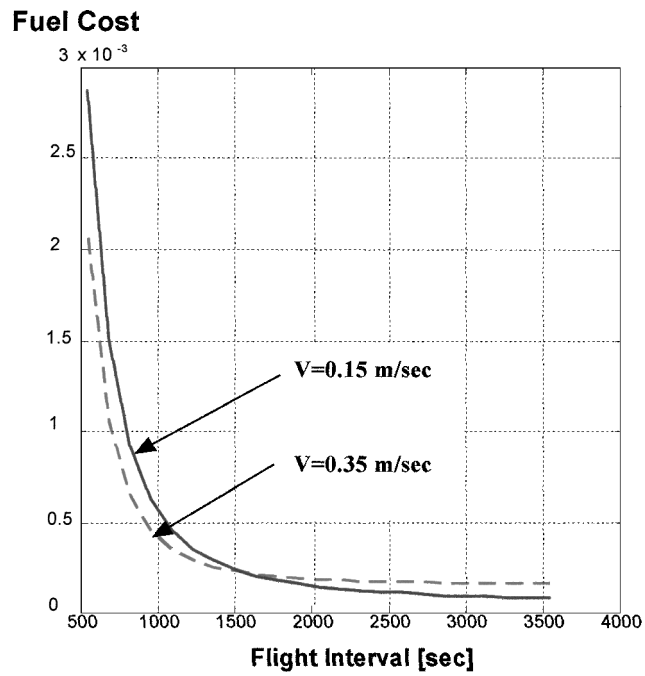

Fig. 14 Second-stage unsaturated fuel cost as a function of second-stage flight interval.

To ensure better controllability margins, unsaturated flight will be required. This requirement implies

$$\max_{t_1 \le t \le t_f} |\boldsymbol{\Gamma}(\boldsymbol{r}_1, |\boldsymbol{v}_1|)| \le \Gamma_{\max} \tag{36}$$

Typically, the global maximum occurs for $t = t_1$ and Eq. (36) can be written as

$$\boldsymbol{\lambda}_1^T \boldsymbol{\lambda}_1 \le \Gamma_{\max}^2 \tag{37}$$

$\Gamma_{\max}^* = \sqrt{(\boldsymbol{\lambda}_1^T \boldsymbol{\lambda}_1)}$ is shown in Fig. 12 for two different values of the intermediate point relative velocity.

As can be seen in Fig. 12 for a sufficiently large flight interval (approximately $\Delta t > 2000$ s) the maximum thrust magnitude becomes a function of spacecraft initial velocity only. The second-stage initial velocity magnitude can be computed from condition (37) to achieve second-stage unsaturated flight.

The second-stage weight coefficient α is defined from terminal approach accuracy requirements. The sensitivity to α is shown in Fig. 13 for a typical case.

During the second stage, additional thrust acceleration is required to maintain the chaser on the final approach line. As the flight interval increases, more fuel is consumed for this purpose. On the other hand, fuel consumed for optimal transfer decreases for increasing flight interval. Thus, starting from a certain flight interval value, we expect no cost improvement. This is clearly seen in Fig. 14, which shows second-stage fuel cost J for the case of unsaturated flight.

Conclusions

The structure of the solution of the fixed-time, linear, low-thrust, fuel-optimal constrained terminal approach-direction rendezvous of a spacecraft with a vehicle in circular orbit has been determined.

A two-stage solution was implemented, formed by a fuel optimal branch to reach an intermediate state on the final approach direction with velocity along the approach line, and a final line-of-sight trajectory branch from the intermediate state to the final approach conditions. This approach provides a solution from all possible initial conditions and achieves the final approach direction from a sufficiently great range. Only marginal additional fuel consumption is required in comparison with the free-approach solution.

Appendix: State and Adjoint Vectors Solution

Solution of the linear system (4) is given in Eq. (18) and repeated here:

$$\boldsymbol{x}(t) = \Phi(t - t_0)\boldsymbol{x}_0 + \Psi(t - t_0)\boldsymbol{\lambda}_0 \tag{A1}$$

Φ is the transition matrix, and Ψ is the convolution integral for the state vector due to the optimal acceleration $\Gamma^*(t)$.

The partitions of the state transition matrix $\Phi(t)$ are defined as follows:

$$\Phi(t) = \begin{bmatrix} \Phi_{11}(t) & \Phi_{12}(t) \\ \Phi_{21}(t) & \Phi_{22}(t) \end{bmatrix} \tag{A2}$$

The individual partitions in normalized units, such that the nominal circular orbit mean motion n is equal to unity, are given by

$$\Phi_{11}(t) = \begin{bmatrix} 1 & 6(t - \sin t) & 0 \\ 0 & 4 - 3\cos t & 0 \\ 0 & 0 & \cos t \end{bmatrix} \tag{A3}$$

$$\Phi_{12}(t) = \begin{bmatrix} 4\sin t - 3t & 2(1 - \cos t) & 0 \\ -2(1 - \cos t) & \sin t & 0 \\ 0 & 0 & \sin t \end{bmatrix} \tag{A4}$$

$$\Phi_{21}(t) = \begin{bmatrix} 0 & 6(1 - \cos t) & 0 \\ 0 & 3\sin t & 0 \\ 0 & 0 & -\sin t \end{bmatrix} \tag{A5}$$

$$\Phi_{22}(t) = \begin{bmatrix} 4\cos t - 3 & 2\sin t & 0 \\ -2\sin t & \cos t & 0 \\ 0 & 0 & \cos t \end{bmatrix} \tag{A6}$$

The convolution integral Ψ can be defined as follows:

$$\Psi(t) = \begin{bmatrix} \Psi_{11}(t) & \Psi_{12}(t) \\ \Psi_{21}(t) & \Psi_{22}(t) \end{bmatrix} \tag{A7}$$

where the elements of the partition are given by

$$\Psi_{11}(t) = \begin{bmatrix} 38\sin t - 10t\cos t + 1.5t^3 - 28t & 16(1 - \cos t) - 5t\sin t - 3t^2 & 0 \\ 16(\cos t - 1) + 5t\sin t + 3t^2 & 6.5\sin t - 2.5t\cos t - 4t & 0 \\ 0 & 0 & 0.5(\sin t - t\cos t) \end{bmatrix} \tag{A8}$$

$$\Psi_{12}(t) = \begin{bmatrix} 28(1 - \cos t) - 10t\sin t - 4.5t^2 & 5t\cos t - 11\sin t + 6t & 0 \\ 11\sin t - 5t\cos t - 6t & 4(1 - \cos t) - 2.5t\sin t & 0 \\ 0 & 0 & -0.5t\sin t \end{bmatrix} \tag{A9}$$

$$\Psi_{21}(t) = \begin{bmatrix} 10t\sin t + 28(\cos t - 1) + 4.5t^2 & 11\sin t - 5t\cos t - 6t & 0 \\ 5t\cos t - 11\sin t + 6t & 4(\cos t - 1) + 2.5t\sin t & 0 \\ 0 & 0 & 0.5t\sin t \end{bmatrix} \tag{A10}$$

$$\Psi_{22}(t) = \begin{bmatrix} 18\sin t - 10t\cos t - 9t & 6 - 5t\sin t - 6\cos t & 0 \\ 6(\cos t - 1) + 5t\sin t & 1.5\sin t - 2.5t\cos t & 0 \\ 0 & 0 & -0.5(t\cos t + \sin t) \end{bmatrix} \tag{A11}$$

The adjoint variables transition matrix $\Phi_\lambda(t)$ is defined as

$$\Phi_\lambda(t) = \begin{bmatrix} \Phi_{\lambda 11}(t) & \Phi_{\lambda 12}(t) \\ \Phi_{\lambda 21}(t) & \Phi_{\lambda 22}(t) \end{bmatrix} \tag{A12}$$

The partition matrices are given by

$$\Phi_{\lambda 11}(t) = \begin{bmatrix} 1 & 0 & 0 \\ 6(\sin t - t) & 4 - 3\cos t & 0 \\ 0 & 0 & \cos t \end{bmatrix} \tag{A13}$$

$$\Phi_{\lambda 12}(t) = \begin{bmatrix} 0 & 0 & 0 \\ 6(1 - \cos t) & -3\sin t & 0 \\ 0 & 0 & \sin t \end{bmatrix} \tag{A14}$$

$$\Phi_{\lambda 21}(t) = \begin{bmatrix} 3t - 4\sin t & -2(1 - \cos t) & 0 \\ 2(1 - \cos t) & -\sin t & 0 \\ 0 & 0 & -\sin t \end{bmatrix} \tag{A15}$$

$$\Phi_{\lambda 22}(t) = \begin{bmatrix} 4\cos t - 3 & 2\sin t & 0 \\ -2\sin t & \cos t & 0 \\ 0 & 0 & \cos t \end{bmatrix} \tag{A16}$$

The matrix Ω defined in Eq. (30) is partitioned as

$$\Omega(t) = \begin{bmatrix} \Omega_{11}(t) & \Omega_{12}(t) \\ \Omega_{21}(t) & \Omega_{22}(t) \end{bmatrix} \tag{A17}$$

with

$$\Omega_{11}(t) = \begin{bmatrix} 3t^3 + 14t + 24t\cos t - 3\sin 2t - 32\sin t & 1.5(\cos 2t - 1) - 3t^2 + 6t\sin t & 0 \\ 1.5(\cos 2t - 1) - 3t^2 + 6t\sin t & 6.5t - 8\sin t + 0.75\sin 2t & 0 \\ 0 & 0 & 0.5t - 0.25\sin 2t \end{bmatrix} \tag{A18}$$

$$\Omega_{12}(t) = \begin{bmatrix} -4.5t^2 - 7 + 4\cos t + 3\cos 2t + 12t\sin t & 1.5\sin 2t - 5t + 8\sin t - 6t\cos t & 0 \\ 1.5\sin 2t + 11t - 14\sin t & 4\cos t - 0.75\cos 2t - 13/4 & 0 \\ 0 & 0 & 0.25(\cos 2t - 1) \end{bmatrix} \tag{A19}$$

$$\Omega_{21}(t) = \begin{bmatrix} 3\cos 2t + 4\cos t + 12t\sin t - 4.5t^2 - 7 & 1.5\sin 2t + 11t - 14\sin t & 0 \\ 1.5\sin 2t - 5t + 8\sin t - 6t\cos t & 4\cos t - 0.75\cos 2t - 13/4 & 0 \\ 0 & 0 & 0.25(\cos 2t - 1) \end{bmatrix} \tag{A20}$$

$$\Omega_{22}(t) = \begin{bmatrix} 3\sin 2t + 19t - 24\sin t & 6\cos t - 4.5 - 1.5\cos 2t & 0 \\ 6\cos t - 4.5 - 1.5\cos 2t & 2.5t - 0.75\sin 2t & 0 \\ 0 & 0 & 0.5t + 0.25\sin 2t \end{bmatrix} \tag{A21}$$

References

[1]Williams, S. N., and Coverstone-Carroll, V., "Benefits of Solar Electric Propulsion for the Next Generation of Planetary Exploration Missions," *Journal of Astronautical Sciences*, Vol. 45, No. 2, 1997, pp. 143–159.

[2]Marec, J. P., *Optimal Space Trajectories*, Elsevier Scientific, New York, 1979, Chap. 15.

[3]Lembeck, C., and Prussing, J., "Optimal Impulsive Intercept with Low-Thrust Rendezvous Return," *Journal of Guidance, Control, and Dynamics*, Vol. 16, No. 3, 1993, pp. 426–433.

[4]Carter, T. E., "Optimal Power-Limited Rendezvous for Linearized Equations of Motion," *Journal of Guidance, Control, and Dynamics*, Vol. 17, No. 5, 1994, pp. 1082–1086.

[5]Pardis, C. J., and Carter, T. E., "Optimal Power-Limited Rendezvous with Thrust Saturation," *Journal of Guidance, Control, and Dynamics*, Vol. 18, No. 5, 1995, pp. 1145–1150.

[6]Kechichian, J. A., "Optimal Low-Thrust Transfer Using Variable Bounded Thrust," International Astronautical Federation, Paper IAF-93A.2.10, Oct. 1993.

[7]Carter, T. E., and Pardis, C. J., "Optimal Power-Limited Rendezvous with Upper and Lower Bounds on Thrust," *Journal of Guidance, Control and Dynamics*, Vol. 19, No. 5, 1996, pp. 1124–1133.

[8]Aleshin, M., and Guelman, M., "Optimal Power Limited Rendezvous with Fixed Terminal Approach Direction," *Proceedings of the 37th Israel Annual Conference on Aerospace Sciences*, Technion—Israel Inst. of Technology, Haifa, Israel, 1997, pp. 463–470.

[9]Clohessy, W. H., and Wiltshire, R. S., "Terminal Guidance System for Satellite Rendezvous," *Journal of the Aerospace Sciences*, Vol. 27, Sept. 1960, pp. 653–658.

[10]Axelrod, A., Guelman, M., and Mishne, D., "Optimal Control of Interplanetary Trajectories Using Electrical Propulsion with Discrete Thrust Levels," AIAA Paper 2000-4138, Aug. 2000.